Improved Analysis and Design of Coupled-Line Phase Shifters

Charles E. Free and Colin S. Aitchison, *Fellow, IEEE*

Abstract—**An analysis of coupled-line microstrip phase shifters is presented which shows that significant differences in theoretical performance are obtained by using an exact analysis in terms of odd and even mode propagation velocities rather than the approach in which the velocities are averaged. Measured data are presented and compared with theory over the frequency range 8–12 GHz and the agreement with theory is good.**

I. Introduction

THE CONFIGURATION of a conventional coupled-line phase shifter is shown in Fig. 1. The circuit introduces a transmission phase change between ports 1 and 2 which is a function of the coupled length, L_c. This form of circuit was employed by Schiffman [1] as part of a broadband 90° phase shifter. However, Schiffman's original work was based on stripline transmission structures, where the odd and even modes propagating along the coupled lines have equal phase velocities. Thus Schiffman was able to make use of the well known expressions for coupled-line filters developed by Jones and Bolljahn [2]. When this type of circuit has been designed in microstrip the same transmission equations are usually quoted, and the unequal odd and even mode velocities averaged to provide, theoretically, a well-behaved characteristic with zero insertion loss at all frequencies. In this paper a more exact analysis is performed, in terms of the independent odd and even mode phase changes along the coupled section and shows that for certain values of the electrical length, L_c, the insertion phase departs significantly from the ideal (average mode velocity) characteristic, and the device presents a significant mismatch at the input port. Some authors, notably Schiek and Kohler [3], have recognized the problem and suggested modifications to the basic design to compensate for the difference in the odd and even mode velocities, but there does not appear to have been any extended theoretical consideration of the simple coupled-line section to show the extent of the problem. There is a further problem which does not appear to have been addressed in the literature, namely that of establishing the actual coupled length that should be in situations where the circuit designer is inhibited from using the familiar chamfered entry by other circuit considerations.

Manuscript received November 14, 1994; revised May 25, 1995.
C. E. Free is with the School of Electronic Engineering, Middlesex University, Bounds Green Road, London N11 2NQ, UK.
C. S. Aitchison is with the Department of Electrical Engineering & Electronics, Brunel University, Uxbridge, Middlesex UB8 3PH, UK.
IEEE Log Number 9413431.

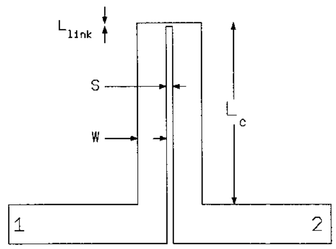

Fig. 1. Configuration of microstrip coupled-line phase shifter.

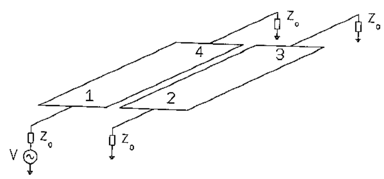

Fig. 2. Coupled microstrip lines showing port configurations.

II. Theory

The method of analysis used here follows the conventional approach adopted for coupled microstrip lines, whereby the total voltages and currents on the structure are obtained from the summation of the odd and even mode solutions. Thus the configuration of the structure shown in Fig. 2 can be reduced to two equivalent circuits as shown in Figs. 3 and 4.

Each of the lines may be analyzed using simple transmission line theory. Thus the currents and voltages at terminals 1 and 4. for the two modes, are related by

$$\begin{bmatrix} V_{1e} \\ I_{1e} \end{bmatrix} = \begin{bmatrix} \cos\theta_e & jZ_{oe}\sin\theta_e \\ jY_{oe}\sin\theta_e & \cos\theta_e \end{bmatrix} \begin{bmatrix} V_{4e} \\ I_{4e} \end{bmatrix} \quad (1)$$

and

$$\begin{bmatrix} V_{1o} \\ I_{1o} \end{bmatrix} = \begin{bmatrix} \cos\theta_o & jZ_{oo}\sin\theta_o \\ jY_{oo}\sin\theta_o & \cos\theta_o \end{bmatrix} \begin{bmatrix} V_{4o} \\ I_{4o} \end{bmatrix} \quad (2)$$

where Z_{oe} and Z_{oo} are the even and odd mode characteristic impedances, and Y_{oe} and Y_{oo} are the corresponding admittances. The relationships between the voltages and currents on the line joining ports 2 and 3 can then be deduced from symmetry. On the microstrip structure being considered, ports 3 and 4 are connected by a narrow conducting link. The link is designed to be narrow so that there will be no propagation around the end of the coupled section, but rather that the even and odd modes will be terminated by open and short circuits, respectively.

0018–9480/95$04.00 © 1995 IEEE

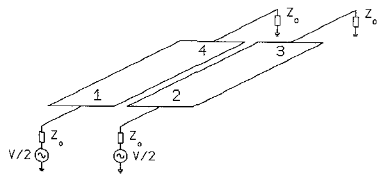

Fig. 3. Even mode equivalent circuit.

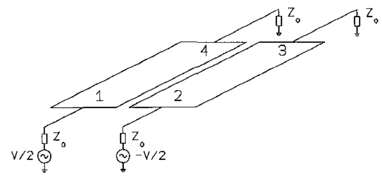

Fig. 4. Odd mode equivalent circuit.

Thus the boundary conditions for the structure may be written as

$$I_{3e} = I_{4e} = 0$$
$$V_{3o} = V_{4o} = 0.$$

The transmission coefficient, V_2/V_1, for the circuit is obtained from

$$\frac{V_2}{V_1} = \frac{V_{2e} + V_{2o}}{V_{1e} + V_{1o}}. \tag{3}$$

It follows, from considerations of symmetry, that the transmission coefficient can also be written as

$$\frac{V_2}{V_1} = \frac{V_{1e} - V_{1o}}{V_{1e} + V_{1o}}$$

giving, after substitution for terminal voltages in terms of line characteristic impedances

$$\frac{V_2}{V_1} = \frac{-jZ_o(Z_{oe} \cot \theta_e + Z_{oo} \tan \theta_o)}{2Z_{oe}Z_{oo} \tan \theta_o \cot \theta_e - jZ_o(Z_{oe} \cot \theta_e - Z_{oo} \tan \theta_o)} \tag{4}$$

from which the transmission phase change is obtained as

$$\phi = \frac{\pi}{2} + \tan^{-1}\left[\frac{Z_o(Z_{oo} \tan \theta_o - Z_{oe} \cot \theta_e)}{2Z_{oe}Z_{oo} \tan \theta_o \cot \theta_e}\right]. \tag{5}$$

(The detailed derivations of (4) and (5) are given in the Appendix.)

If it is assumed that the odd and even modes have equal phase velocities, i.e., $\theta_o = \theta_e = \theta$, then (5) reduces to

$$\phi = \cos^{-1}\left[\frac{\dfrac{Z_{oe}}{Z_{oo}} - \tan^2 \theta}{\dfrac{Z_{oe}}{Z_{oo}} + \tan^2 \theta}\right] \tag{6}$$

which is the form quoted by Schiffman, and usually employed as an approximation in microstrip designs.

The approximations usually made in coupled-line phase shifters also extend to the match of the circuit, wherein it is assumed that the input impedance is given by

$$Z_o = \sqrt{Z_{oe}Z_{oo}}.$$

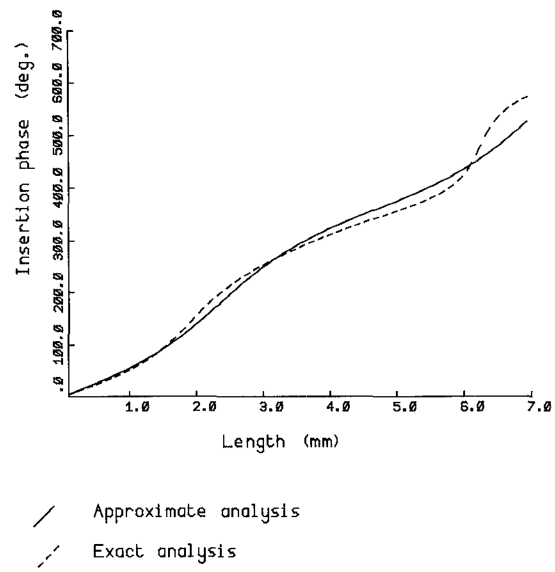

Fig. 5. Theoretical insertion phase at 12 GHz.

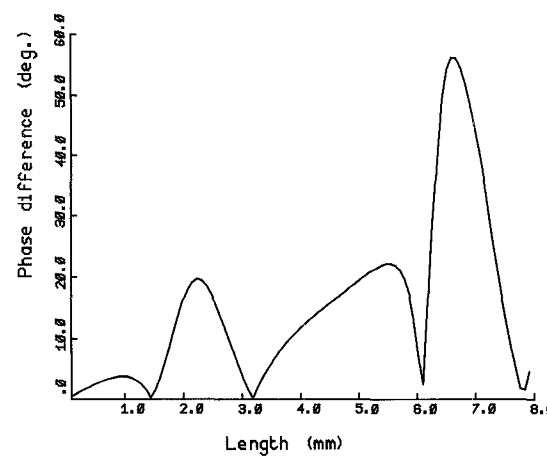

Fig. 6. Difference between exact and approximate theoretical insertion phase at 12 GHz.

It is shown in the Appendix that if the exact analysis is employed the input impedance at port 1 is frequency dependent and given by

$$Z_1 = \frac{2Z_{oe}Z_{oo} \cot \theta_e \tan \theta_o - jZ_o(Z_{oe} \cot \theta_e - Z_{oo} \tan \theta_o)}{2Z_o - j(Z_{oe} \cot \theta_e - Z_{oo} \tan \theta_o)}. \tag{7}$$

III. Comparison of Exact and Approximate Theory

Fig. 5 shows the theoretical insertion phase, computed as a function of the coupler length at 12 GHz, which results from using the approximate and exact methods of analysis. It can be seen that the exact response departs significantly from the approximate characteristic for certain lengths and, as would be expected, the difference tends to increase with the length of the coupled section. This is demonstrated more clearly in Fig. 6, where the magnitude of the of the difference between the responses has been plotted as a function of the length, and shows that the difference can be as large as 60°.

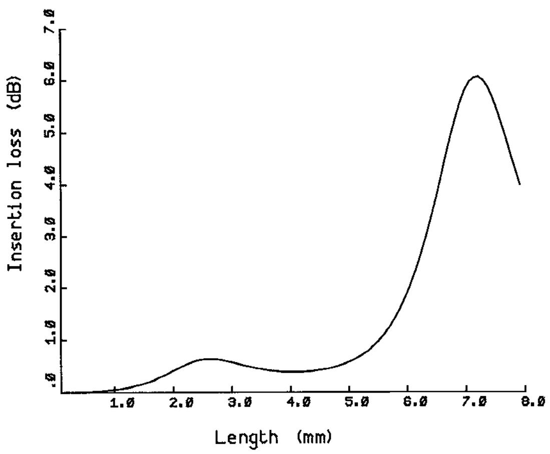

Fig. 7. Theoretical insertion loss for phase shifter at 12 GHz using exact analysis.

The approximate theory assumes that the match of the circuit is perfect, and frequency invariant. It can be seen from Fig. 7 that the exact analysis predicts significant insertion loss, due to circuit mismatch. As would be expected the highest loss occurs in the same region as the highest phase difference.

IV. Practical Design

In order to establish the validity of the new theory a number of coupled-line phase shifters of arbitrary length were designed and tested at X-band. The coupled-line geometry was chosen to give nominal input and output port impedances of 50 Ω, using $Z_o = (Z_{oe} Z_{oo})^{0.5}$. There is no unique combination of track width (w) and spacing (s) to satisfy this relationship and the actual values were selected so as to make the fabrication relatively noncritical. In calculating the values of θ_e and θ_o the Getsinger [4] model was used to account for dispersive effects. The effective length of the coupled region for the even mode was taken to be $L_c + l_{eo}$, where l_{eo} represents the effect of fringing at the remote end of the coupler and was evaluated from the well-known expression due to Hammerstad and Bekkadal [5]. In calculation for l_{eo} the effective width of the line was taken to be $2w + s$. Since the odd mode is fairly precisely terminated by the link between ports 3 and 4 no allowance was made for fringing, other than to use the full value of L_c, including L_{link}, for the odd mode on the basis that there will be some slight extension of the of the odd mode length due to the effective inductance caused by the odd mode penetrating into the narrow link.

V. Circuit Data

The test circuits were fabricated on RT/duroid 6010 having a substrate thickness of 635 μm, a track thickness of 4.5 μm, and a relative permittivity of 10.4. The actual dimensions of the circuits tested are given in Table I.

VI. Comparison of Practical Measurements with Theory

In Figs. 8–12 comparisons are presented between the theoretical insertion phase and measured data over the X-band frequency range for five couplers with different lengths. The lengths of the couplers were chosen to cover a wide range of phases, in arbitrary steps. The error bars associated with the measured data show a ±1° measurement uncertainty. It can be seen that in all cases there is good agreement between the measured data and the predicted response based on an exact analysis. For circuit 1, with the shortest coupled length, the agreement is particularly good with the exact response well within the 1° error bounds of the measured data. For the other responses, even when the exact response lies outside the measured data error bounds the departure is small compared to the difference between the exact and approximate values. The agreement between the measured data and the exact response is emphasized by considering the shape of the responses. There are significant differences between the shapes of the approximate and exact responses, particularly for the longer coupled lengths, but in all cases the measured data points follow closely the shape of the exact response.

TABLE I
Test Circuit Dimensions [μm]—The Symbols are Defined in Fig 1

CIRCUIT	L_c	L_{link}	w	s
1	759	26	465	100
2	1257	47	476	95
3	1784	30	470	103
4	4650	52	477	109
5	6672	54	469	109

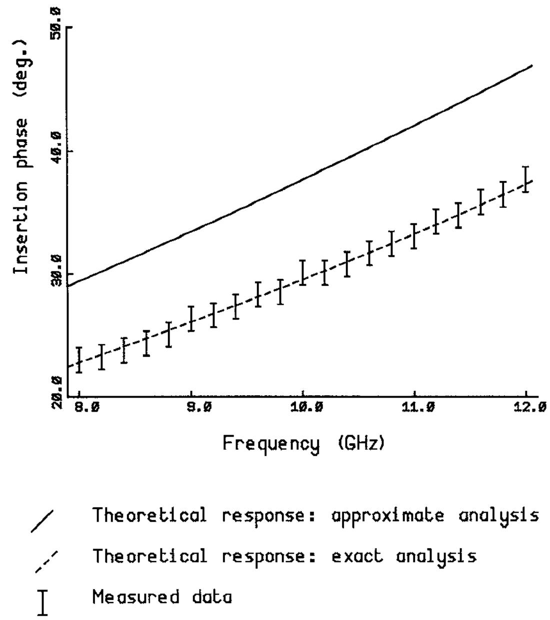

Fig. 8. Comparison of measured and theoretical data for circuit 1.

Figs. 11 and 12, which represent the longer coupled sections, show that the agreement between measured data and the exact response tends to worsen at the top end of the frequency band. This suggests that some dispersive effect is involved, which would naturally increase with the length of the coupled section. Getsinger's mode [4] was used to account for dispersion, but some authors, notably Easter and Gupta [6], have suggested that this model gives a slight overestimate of the effect of dispersion. This would be consistent with the results shown in

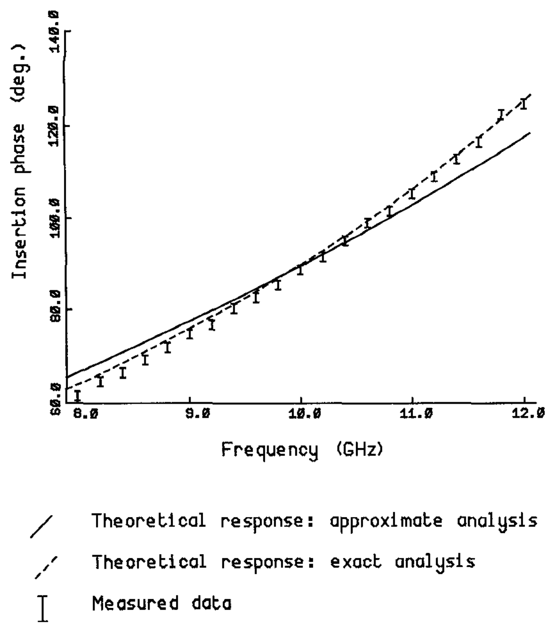

Fig. 9. Comparison of measured and theoretical data for circuit 2.

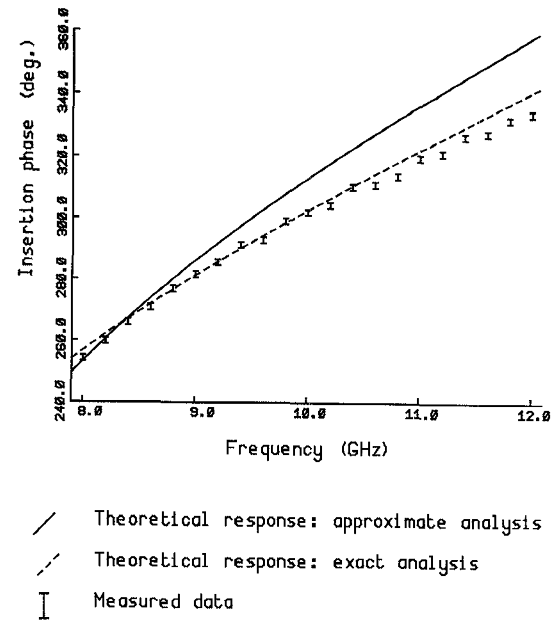

Fig. 11. Comparison of measured and theoretical data for circuit 4.

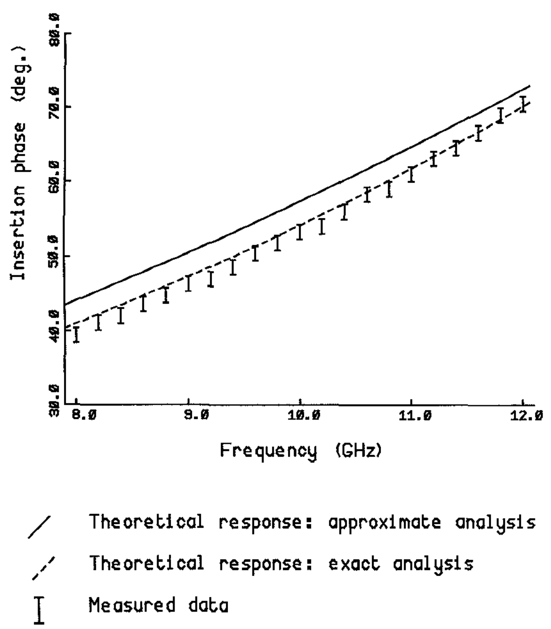

Fig. 10. Comparison of measured and theoretical data for circuit 3.

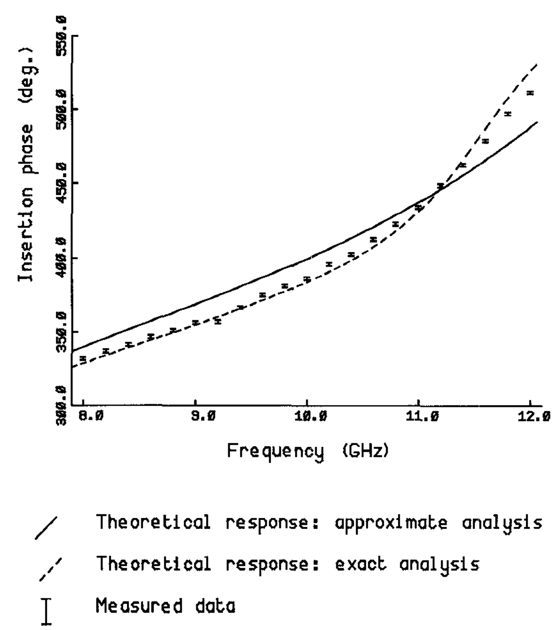

Fig. 12. Comparison of measured and theoretical data for circuit 5.

Figs. 11 and 12, where the predicted insertion phase is slightly higher than the measured data at the top end of the band. A more recent dispersion model, from Kirshning and Jansen [7], claims to provide a more accurate prediction of dispersion effects at higher microwave frequencies, and could possibly improve the fit between the measured data and exact theory in the 11–12 GHz region.

VII. Bend Discontinuity

In calculating the theoretical responses no attempt was made to model the discontinuities formed by the 90° bends at the entry to the coupled region; indeed, there do not appear to exist in the literature discontinuity models which include the combined effects of bends and coupling. However, it would appear from the results that this is an unnecessary refinement for the circuit designer and that adequate prediction of the insertion phase results from using the nominal length, L_c, together with small compensations for fringing at the remote end of the device.

It is not thought that the bend discontinuity contributed to the departure of the measured data from the exact response at the higher end of the measured band, since this effect was only noticeable for the longer coupled sections and suggested a purely length dependent effect.

VIII. Application

While the insertion phase exhibits some degree of nonlinearity with frequency, the simple coupled-line section, without the changes in line geometry which have been introduced by some authors [3], still offers a useful and easily fabricated microstrip circuit component, which can yield very predictable results, based on an exact analysis. Moreover, its simple geometry would seem to be attractive for use at higher microwave frequencies where changes in line geometry, introduced for mode velocity compensation, would themselves introduce significant discontinuities.

IX. Conclusion

It has been shown that an exact analysis method is needed to satisfactorily predict the performance of coupled-line phase shifters and, moreover, that the device exhibits a significant mismatch under certain conditions. A comparison between measured and theoretical data shows that the new theory, based on an exact method of analysis in terms of the independent odd and even mode velocities, provides a better prediction of the nonlinear phase responses which are observed in practice.

Useful information has also been obtained on the effective length of the coupler which should be employed in practical designs.

Appendix
Exact Analysis of Coupled-Line Phase Shifter

Equation (1) can be expanded to give

$$V_{1e} = V_{4e} \cos\theta_e + jI_{4e} Z_{oe} \sin\theta_e \quad \text{(A1)}$$
$$I_{1e} = jV_{4e} Y_{oe} \sin\theta_e + I_{4e} \cos\theta_e \quad \text{(A2)}$$

and similarly (2) gives

$$V_{1o} = V_{4o} \cos\theta_o + jI_{4o} Z_{oo} \sin\theta_o \quad \text{(A3)}$$
$$I_{1o} = jV_{4o} Y_{oo} \sin\theta_o + I_{4o} \cos\theta_o. \quad \text{(A4)}$$

The boundary conditions are

$$V_{4o} = V_{3o} = 0$$
$$I_{4e} = I_{3o} = 0.$$

Substituting the boundary conditions into (A1)–(A4) gives

$$V_{1e} = V_{4e} \cos\theta e \quad \text{(A5)}$$
$$I_{1e} = jV_{4e} Y_{oe} \sin\theta_e \quad \text{(A6)}$$

and

$$V_{1o} = jI_{4o} Z_{oo} \sin\theta_o \quad \text{(A7)}$$
$$I_{1o} = I_{4o} \cos\theta_o. \quad \text{(A8)}$$

The input impedance at port 1 is given by

$$\begin{aligned} Z_{\text{in},1} &= \frac{V_{1e}+V_{1o}}{I_{1e}+I_{1o}} \\ &= \frac{V_{1e}+V_{1o}}{jV_{4e}Y_{oe}\sin\theta_e + I_{4o}\cos\theta_o} \\ &= \frac{V_{1e}+V_{1o}}{j\dfrac{V_{1e}}{\cos\theta_e}Y_{oe}\sin\theta_e + \dfrac{V_{1o}}{jZ_{oo}\sin\theta_o}\cos\theta_o} \\ &= \frac{V_{1e}+V_{1o}}{j(V_{1e}Y_{oe}\tan\theta_e - V_{1o}Y_{oo}\cot\theta_o)}. \end{aligned} \quad \text{(A9)}$$

Now, if Z_{1e} and Z_{1o} are the input impedances at port 1 for the even and odd modes, respectively, then

$$V_{1e} = \frac{Z_{1e}}{Z_{1e}+Z_o}\frac{V}{2} \quad \text{(A10)}$$
$$V_{1o} = \frac{Z_{1o}}{Z_{1o}+Z_o}\frac{V}{2}. \quad \text{(A11)}$$

Also, from (A5) and (A6)

$$Z_{1e} = \frac{V_{1e}}{I_{1e}} = -jZ_{oe}\cot\theta_e \quad \text{(A12)}$$

and

$$Z_{1o} = \frac{V_{1o}}{I_{1o}} = jZ_{oo}\tan\theta_o. \quad \text{(A13)}$$

Substituting from (A10)–(A13) into (A9) we obtain, after straightforward manipulation, (A14) as shown at the bottom of the page.

The input reflection coefficient, S_{11}, is given by

$$S_{11} = \frac{Z_{\text{in},1}-Z_o}{Z_{\text{in},1}+Z_o}. \quad \text{(A15)}$$

It should be noted that if we put $\theta_e = \theta_o = \theta$, the expression for $Z_{\text{in},1}$ becomes

$$Z_{\text{in},1} = \frac{2Z_{oe}Z_{oo} - jZ_o(Z_{oe}\cot\theta - Z_{oo}\tan\theta)}{2Z_o - j(Z_{oe}\cot\theta - Z_{oo}\tan\theta)} \quad \text{(A16)}$$

and then, if

$$Z_o = \sqrt{Z_{oe}Z_{oo}}$$

we obtain

$$Z_{\text{in},1} = Z_o$$

which is the nominal matched condition.

The transmission coefficient representing transmission between ports 1 and 2 is given by

$$\frac{V_2}{V_1} = \frac{V_{2e}+V_{2o}}{V_{1e}+V_{1o}}. \quad \text{(A17)}$$

$$Z_{\text{in},1} = \frac{2Z_{oe}Z_{oo}\cot\theta_e\tan\theta_o - jZ_o(Z_{oe}\cot\theta_e - z_{oo}\tan\theta_o)}{2Z_o - j(Z_{oe}\cot\theta_e - Z_{oo}\tan\theta_o)}. \quad \text{(A14)}$$

$$\frac{V_2}{V_1} = -j\frac{Z_o(Z_{oe}\cot\theta_e - Z_{oo}\tan\theta_o)}{2Z_{oe}Z_{oo}\tan\theta_o\cot\theta_e - jZ_o(Z_{oe}\cot\theta_e - Z_{oo}\tan\theta_o)}. \quad \text{(A19)}$$

From considerations of symmetry, (A17) can be written as

$$\frac{V_2}{V_1} = \frac{V_{1e} - V_{1o}}{V_{1e} + V_{1o}} = \frac{\dfrac{Z_{1e}}{Z_{1e} + Z_o} - \dfrac{Z_{1o}}{Z_{1o} + Z_o}}{\dfrac{Z_{1e}}{Z_{1e} + Z_o} + \dfrac{Z_{1o}}{Z_{1o} + Z_o}}. \tag{A18}$$

Thus, substituting from (A12) and (A13) we obtain (A19) as shown at the bottom of the preceding page.

From (A19) the transmission phase change is obtained as

$$\phi = \frac{\pi}{2} + \tan^{-1}\left[\frac{Z_o(Z_{oe}\cot\theta_e - Z_{oo}\tan\theta_o)}{2Z_{oe}Z_{oo}\tan\theta_o\cot\theta_e}\right]. \tag{A20}$$

This is the exact expression for insertion phase. We can simplify this by making assumptions about Z_{oe} and Z_{oo} and by letting $\theta_e = \theta_o = \theta$. We have already established that the approximate theory, averaging the odd and even mode velocities, yields a matched input condition when

$$z_o = \sqrt{Z_{oe}Z_{oo}}.$$

Substituting these simplifying conditions into (A20) gives

$$\phi = \frac{\pi}{2} + \tan^{-1}\left[\frac{Z_{oe}\cot\theta - Z_{oo}\tan\theta}{2\sqrt{Z_{oe}Z_{oo}}}\right] \tag{A21}$$

whence

$$\cot\phi = \frac{Z_{oo}\tan\theta - Z_{oe}\cot\theta}{2\sqrt{Z_{oe}Z_{oo}}}.$$

Using the trigonometric relationship

$$\cot^2\phi = \frac{\cos^2\phi}{1 - \cos^2\phi}$$

we obtain

$$\cos\phi = \pm\frac{Z_{oo}\tan\theta - Z_{oe}\cot\theta}{Z_{oo}\tan\theta + Z_{oe}\cot\theta}.$$

Now we know

$$\phi = 0 \quad \text{when} \quad \theta = 0$$

hence

$$\cos\phi = \frac{\dfrac{Z_{oe}}{Z_{oo}} - \tan^2\theta}{\dfrac{Z_{oe}}{Z_{oo}} + \tan^2\theta}$$

or

$$\phi = \cos^{-1}\left[\frac{\rho - \tan^2\theta}{\rho + \tan^2\theta}\right] \tag{A22}$$

where

$$\rho = \frac{Z_{oe}}{Z_{oo}}.$$

Equation (A22) thus gives the approximate insertion phase of the coupler which should be employed in practical designs.

References

[1] B. M. Schiffman, "A new class of broadband microwave 90° phase shifters," *IRE Trans.*, vol. MTT-6, no. 4, pp. 232–237, Apr. 1958.

[2] E. M. T. Jones and J. T. Bolljahn, "Coupled-strip transmission line filters and directional couplers," *IRE Trans.*, vol. MTT-4, no. 4, pp. 124–130, Apr. 1956.

[3] B. Schiek and J. Kohler, "A method for broadband matching of differential phase shifters," *IEEE Trans. Microwave Theory Tech.*, vol. MTT-25, no. 8, pp. 666–671, Aug. 1977.

[4] W. J. Getsinger, "Microstrip dispersion model," *IEEE Trans. Microwave Theory Tech.*, vol. 21, no. 1, pp. 34–39, Jan. 1993.

[5] E. O. Hammerstad and F. Bekkadal, "A microstrip handbook," *ELAB Report STF 44A74169, N7034*, Univ. of Trondheim—NTH, Norway 1975.

[6] B. Easter and K. C. Gupta, "More accurate model of coupled microstrip line section," *IEEE J. Microwaves, Optics and Acoustics*, vol. 3, no. 3, pp. 99–103, May 1973.

[7] M. Kirschning and R. H. Jansen, "Accurate wide-range design equations for the frequency—dependent characteristics of parallel coupled microstrip lines," *IEEE Trans. Microwave Theory Tech.* vol. MTT-32, no. 1, pp. 83–90, Jan. 1984.

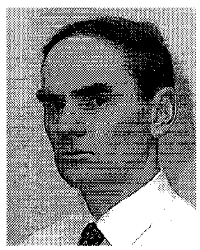

Charles E. Free received the B.Sc. in electrical engineering from Aston University in the UK and the M.Sc. in communication systems.

He worked as a Research Engineer on Q-band communications at Marconi Research Centre, Great Baddow, England. He is now a Principal Lecturer in electronic communications at Middlesex University, London, where his research interests are mainly in microwave circuits and propagation.

Colin S. Aitchison (SM'90–F'94) received the B.Sc. from Imperial College in London in 1955.

He joined Philips Research Laboratories where he ran a research group concerned with novel microwave active components including parametric amplifiers and other solid state circuits. In 1972 he joined Chelsea College, University of London, and became Professor and Head of Department extending his research interests to include distributed amplifiers. In 1984 he joined ERA Technology to establish an active microwave research group concerned with distributed amplifiers, systems, and microwave power amplifiers. In 1989 he joined Brunel University continuing with his active research activities. He is currently Professor and Head of Department. He has published 120 papers.

Mr. Aitchison is a Fellow of the IEEE and IEE.